The output of Hedgehog signaling is controlled by the dynamic association between Suppressor of Fused and the Gli proteins

Eric W. Humke,[1] Karolin V. Dorn,[1] Ljiljana Milenkovic,[2,3,4,5] Matthew P. Scott,[2,3,4,5] and Rajat Rohatgi[1,6]

[1]Division of Oncology, Department of Medicine, Stanford University School of Medicine, Stanford, California 94305, USA; [2]Department of Developmental Biology, Stanford University School of Medicine, Stanford, California 94305, USA; [3]Department of Genetics, Stanford University School of Medicine, Stanford, California 94305, USA; [4]Department of Bioengineering, Stanford University School of Medicine, Stanford, California 94305, USA; [5]Howard Hughes Medical Institute, Stanford University School of Medicine, Stanford, California 94305, USA

The transcriptional program orchestrated by Hedgehog signaling depends on the Gli family of transcription factors. Gli proteins can be converted to either transcriptional activators or truncated transcriptional repressors. We show that the interaction between Gli3 and Suppressor of Fused (Sufu) regulates the formation of either repressor or activator forms of Gli3. In the absence of signaling, Sufu restrains Gli3 in the cytoplasm, promoting its processing into a repressor. Initiation of signaling triggers the dissociation of Sufu from Gli3. This event prevents formation of the repressor and instead allows Gli3 to enter the nucleus, where it is converted into a labile, differentially phosphorylated transcriptional activator. This key dissociation event depends on Kif3a, a kinesin motor required for the function of primary cilia. We propose that the Sufu–Gli3 interaction is a major control point in the Hedgehog pathway, a pathway that plays important roles in both development and cancer.

[*Keywords*: Hedgehog signaling; Gli proteins; Suppressor of Fused; primary cilia; development; cancer]

Supplemental material is available at http://www.genesdev.org.

Received January 7, 2010; revised version accepted February 19, 2010.

The Hedgehog (Hh) signaling pathway regulates cell proliferation, differentiation, and patterning in a range of tissues during animal development. The overall structure of the Hh pathway, first elucidated in *Drosophila*, is composed of a series of repressive interactions (Varjosalo and Taipale 2008). In the absence of a signal, target gene transcription is shut off by the transmembrane protein Patched 1 (Ptc1). Ptc1 inhibits the function of a seven-pass transmembrane protein, Smoothened (Smo). The pathway is activated by a secreted Hh protein in flies, and one of three proteins—Sonic Hedgehog (Shh), Indian Hh, and Desert Hh—in mammals. Shh binds and inactivates Ptc1 with the help of coreceptors, thus releasing Smo from inhibition. The ultimate consequence of Smo activation is production of activating forms of the Hh transcription factors: Cubitus Interruptus (Ci) in flies, and three Gli proteins (Gli1–3) in mammals. Ci exists in two forms: a full-length transcriptional activator (Ci155), and a truncated N-terminal fragment that functions as a repressor (Ci75). Hh suppresses the formation of Ci75 and promotes the conversion of Ci155 into a transcriptional activator (Ci155A). The functions of Ci are distributed among the three Gli proteins in mammals. Gli2 and Gli3 exist in both full-length (FL) and repressor (R) forms, although Gli2 is considered primarily a transcriptional activator (A). Gli3 most closely resembles Ci155 in having dual repressor and activator functions. *Gli1* is an early transcriptional target of Hh signaling and functions exclusively as a transcriptional activator. Hh signaling shapes the transcriptional response of a cell by altering the ratio of activator and repressor functions of the Gli proteins. Understanding the conversion of Gli proteins into activator and repressor forms is essential for understanding the Hh pathway in normal physiology, and for controlling it in pathological states.

Full-length Ci and Gli3 have two biochemical fates that are regulated by Hh signaling. A large amount of mechanistic information is available about how Gli3FL and Ci155 are converted to transcriptional repressors (Gli3R and Ci75) in the absence of Shh (Aza-Blanc et al. 1997;

[6]**Corresponding author.**
E-MAIL rrohatgi@stanford.edu; FAX (650) 725-6044.
Article is online at http://www.genesdev.org/cgi/doi/10.1101/gad.1902910.

Methot and Basler 1999; Wang et al. 2000). In flies and mammals, protein kinase A (PKA) initiates a phosphorylation cascade in which PKA, glycogen synthase kinase 3 (GSK3), and casein kinase 1 (CK1) phosphorylate Gli3FL and Ci155 (Zhang et al. 2005; Tempe et al. 2006; Wang and Li 2006; Smelkinson et al. 2007). Phosphorylation targets Gli3 for ubiquitination and limited processing by the proteasome into an N-terminal repressor fragment (Gli3R). In flies, Hh inhibits Ci75 formation by causing dissociation of kinases from Ci155 and reducing Ci155 phosphorylation (Chen et al. 1999; Zhang et al. 2005). The mechanism by which Hh inhibits Gli3R formation has not been established in mammals. In the presence of Shh, Gli3FL and Ci155 are converted into full-length transcriptional activator proteins (Gli3A or Ci155A). The biochemical mechanism of this activation process remains mysterious in both flies and mammals.

The regulation of Ci and Gli proteins in response to Smo activation has diverged significantly between mammals and flies. In flies, this regulation depends on a complex of three proteins: the kinase Fused, the protein Suppressor of Fused (Sufu), and the atypical kinesin Costal 2 (Cos2). Cos2 recruits the kinases PKA, GSK3, and CK1 to phosphorylate Ci155 and promote the formation of Ci75 (Zhang et al. 2005). When Hh is received, the Cos2 scaffolded complex is recruited to the Smo C-terminal tail (Lum et al. 2003), an interaction that inhibits Ci75 formation. Higher doses of Hh can promote conversion of Ci155 into the active Ci155A by an unknown reaction that depends on the kinase Fused (Ohlmeyer and Kalderon 1998; Wang and Holmgren 1999; Methot and Basler 2000). A requirement for Sufu is seen only in Fused mutants, implying that Sufu is not absolutely required in flies for regulation of Hh signaling (Preat 1992).

In mammals, Gli regulation depends on the primary cilium, a solitary cell surface projection that functions as a major signaling center in the cell. Disruption of intraflagellar transport (IFT), the motor-driven transport mechanism that moves proteins along the cilium, prevents formation of Gli3R and reduces Gli2/3A function in embryos (Huangfu et al. 2003; Huangfu and Anderson 2005; Liu et al. 2005). Most proteins in the Hh pathway, including Ptc1, Smo, Sufu, and the Gli proteins, localize to cilia, and it is likely that many of the critical reactions in the pathway occur within this specialized compartment (Corbit et al. 2005; Haycraft et al. 2005; Rohatgi et al. 2007).

In sharp contrast to its ancillary role in flies, Sufu plays a crucial negative role in mammalian Hh signaling. Genetic inactivation of Sufu leads to constitutive activation of Hh target genes in cultured cells and in mice (Cooper et al. 2005; Svard et al. 2006). In humans, *Sufu* is a tumor suppressor gene; its inactivation can cause medulloblastomas and the Gorlin's syndrome tumors (Taylor et al. 2002; Pastorino et al. 2009). Sufu binds directly to the Gli proteins (Pearse et al. 1999; Stone et al. 1999), but we do not understand how Sufu antagonizes the function of the Gli proteins or how Hh signaling antagonizes Sufu to unleash Gli activity. Previous studies have suggested two roles for Sufu: tethering Gli proteins in the cytoplasm, or suppressing Gli transcriptional activity in the nucleus. The literature has conflicting reports on the relative importance of these mechanisms (Ding et al. 1999; Cheng and Bishop 2002; Svard et al. 2006). The ability of Sufu to inhibit signaling is preserved in cells lacking IFT components, so Sufu function is probably independent of primary cilia (Chen et al. 2009; Jia et al. 2009). Cells lacking Sufu contain very low steady-state levels of Gli2, Gli3FL, and Gli3R, raising the question of how these cells attain a high level of Hh target gene transcription (Chen et al. 2009; Jia et al. 2009).

In this study, we present experiments designed to illuminate the final steps along the path of Hh signal transduction—the regulation of GliA and GliR functions by Sufu. We focused our attention on Gli3 because it behaves most like the fly Ci protein. Our experimental approach is based on the analysis of endogenous proteins and their interactions in cultured fibroblasts in response to acute activation of Hh signaling, thus avoiding the pitfalls of overexpressed proteins or cells undergoing long-term adaptation to constitutive signal transduction. We find that the association of Sufu and Gli3 is regulated by Hh signaling, and that this critical interaction controls the balance between Gli3R versus Gli3A formation.

Results

Acute Hh pathway activation causes a decline in the stability of Gli3FL

Using antibodies that recognize endogenous Gli1, Gli3, or Ptc1, we assessed levels of these proteins in lysates from NIH3T3 fibroblasts treated with Shh (Fig. 1A). The antibody used to detect Gli3 recognized both Gli3FL and Gli3R, since it was directed against a common epitope in the N terminus of Gli3. *Gli1* and *Ptc1* are two early target genes induced by Hh signaling, and the levels of their protein and RNA products (Fig. 1A,B) increased in a time-dependent manner. As observed previously, Gli3R protein levels declined in response to Shh (Fig. 1A; Wang et al. 2000). Current models predict that this decline in Gli3R should be accompanied by a concomitant increase in its precursor, Gli3FL. Instead, we found that Gli3FL protein levels also decreased in response to Shh (Fig. 1A). The decrease in Gli3 levels in response to Shh was inhibited by SANT-1, a small molecule antagonist of Smo (Supplemental Fig. S1A). Control experiments ensured that both forms of Gli3 were extracted efficiently from cells (Supplemental Fig. S1B).

To confirm this surprising concordant reduction in Gli3FL and Gli3R, cells were treated with Shh in the presence of increasing concentrations of Forskolin (Fsk). Fsk, an activator of adenylate cyclase (AC), can inhibit Hh signaling and induce formation of Gli3R because it activates PKA by raising cellular cAMP levels (Wang et al. 2000). Fsk inhibited Hh signaling in a dose-dependent manner, assayed by Gli1 protein levels (Fig. 1C). This inhibition was accompanied by increases in both Gli3FL and Gli3R protein levels (Fig. 1C,D). Thus, both acute pathway activation by Shh and inactivation by Fsk led to

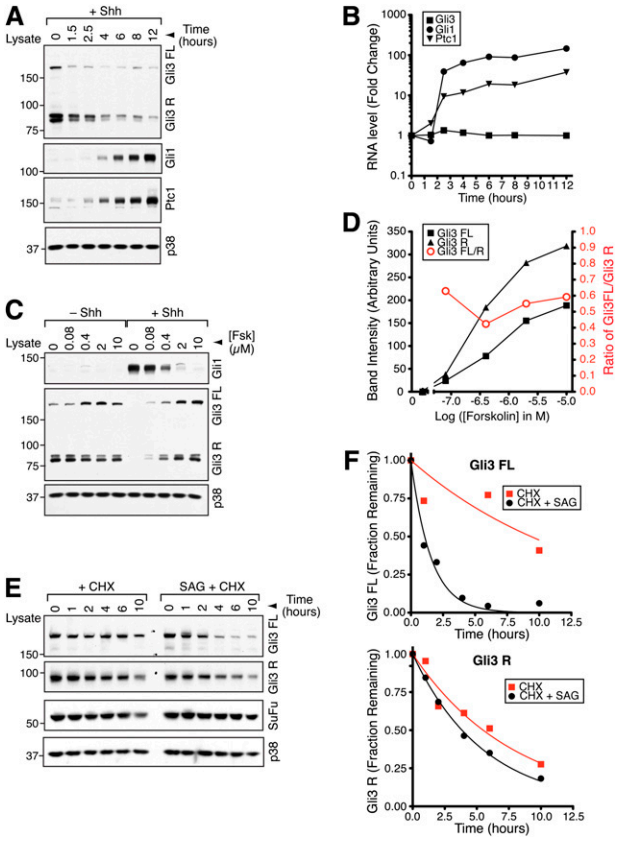

Figure 1. Hh signaling decreases the stability of Gli3FL but not Gli3R. (*A*,*B*) NIH3T3 cells were treated with Shh, and levels of Gli3FL, Gli3R, Gli1, and Ptc1 protein (*A*) and RNA (*B*) were assayed by immunoblotting and quantitative RT–PCR, respectively. Levels of *Gli1* and *Ptc1*, two Hh target genes, served as a metric of pathway activation, and the p38 protein was a loading control. (*C*,*D*) Levels of Gli1, Gli3FL, Gli3R, and p38 proteins in lysates of NIH3T3 cells treated with Fsk alone at the indicated concentrations or Shh + Fsk for 11 h. Protein levels quantitated by densitometry were plotted in *D*, along with the ratio of the Gli3FL/Gli3R signal (red). (*E*,*F*) Gli3FL, Gli3R, Sufu, and p38 protein levels in NIH3T3 cells treated with cycloheximide (CHX; 100 μg/mL) alone or cycloheximide plus SAG (CHX + SAG; 100 nM) for the indicated periods of time. Different exposures were needed for Gli3FL and Gli3R to avoid saturation of the signal; equivalent exposures are shown in Supplemental Figure S1A. The fraction of Gli3FL and Gli3R remaining (cf. $t = 0$) is plotted in *F*.

concordant changes in Gli3FL and Gli3R. In contrast to prior expectations (Wang et al. 2000), the commonly reported Gli3FL/Gli3R ratio showed little change (Fig. 1D), and so did not serve as a good metric of Hh pathway activity under conditions of acute pathway activation.

These results show that the regulation of Gli3FL levels by Shh cannot occur solely at the Gli3FL → Gli3R conversion step, since this would lead to inverse changes in the levels of the two proteins. The rapid reduction in Gli3FL protein suggested a post-transcriptional mechanism for its regulation. In fact, *Gli3* mRNA did not change significantly during the course of the experiment (Fig. 1B). To exclude a role for synthesis in the regulation of Gli3FL, cycloheximide chase experiments were used to measure the half-life of Gli3FL in response to activation of Hh signaling. Since we were focused on events downstream from Smo and wanted to exclude confounding effects caused by feedback mechanisms that may operate upstream of Smo, we used the direct Smo activator SAG (Smo Agonist) (Chen et al. 2002). Smo activation by SAG reduced the half-life of Gli3FL but did not significantly change the half-life of Gli3R (Fig. 1E,F; Supplemental Fig. S1C). Thus, Hh signaling decreased levels of Gli3FL and Gli3R in fundamentally different ways: It induced the destabilization of Gli3FL, but it inhibited the production of Gli3R without affecting its stability.

Sufu stabilizes Gli3FL

Recent studies have shown that steady-state levels of Gli3FL and Gli3R are very low in *sufu*$^{-/-}$ embryos and cells (Chen et al. 2009; Jia et al. 2009). We asked if Sufu plays a role in regulating the synthesis or the degradation of Gli3FL. *Sufu*$^{-/-}$ cells were infected with a retrovirus carrying a gene for wild-type Sufu (*sufu*$^{-/-}$:Sufu cells) or with an empty retrovirus (*sufu*$^{-/-}$:vector cells). Since Sufu is a negative regulator of the pathway, *sufu*$^{-/-}$:vector cells showed high levels of *Gli1* target gene expression (Fig. 2A). The reintroduction of Sufu or YFP-tagged Sufu extinguished signaling, suppressed Gli1 levels, and restored sensitivity of the cells to pathway activation (Fig. 2A). Compared with control cells, the steady-state levels of Gli3FL and Gli3R were much higher in *sufu*$^{-/-}$:Sufu cells, showing that functional Sufu caused an accumulation of both forms of Gli3. We also confirmed that the endogenous Gli3 protein could form a complex with the reintroduced Sufu (Fig. 2B). Thus, the Sufu added back into *sufu*$^{-/-}$ cells was functional because it interacted with Gli3 and suppressed target gene transcription.

To determine if the difference in Gli3 levels in the presence or absence of Sufu was caused by a difference in synthesis or degradation, cycloheximide was used to block protein synthesis in *sufu*$^{-/-}$:vector cells and *sufu*$^{-/-}$:Sufu cells. The half-life of Gli3FL was drastically shorter (<30 min) in the absence of Sufu compared with the presence of Sufu (>8 h) (Fig. 2C,D; Supplemental Fig. S2A). Gli3FL degradation in cells lacking Sufu was likely mediated by the proteasome, since the addition of epoxomycin, a proteasome inhibitor, increased the steady-state levels of Gli3FL (Fig. 2E).

Sufu potentiates the formation of Gli3R

The low steady-state levels of Gli3R seen in *sufu*$^{-/-}$ cells could result from Sufu driving production of Gli3R, or because Sufu protects Gli3R from degradation. While steady-state levels of Gli3R were different (Fig. 2A), the half-life of Gli3R was identical in *sufu*$^{-/-}$:vector and *sufu*$^{-/-}$:Sufu cells (Figs. 2C, 3A; Supplemental Fig. S2A). Thus, Gli3FL was much more labile than Gli3R in the absence of Sufu (Supplemental Fig. S3A,B). In addition, the steady-state level of a Myc-tagged Gli3R protein introduced into *sufu*$^{-/-}$ cells by transfection did not increase when cotransfected with Sufu (Fig. 3B). Taken together,

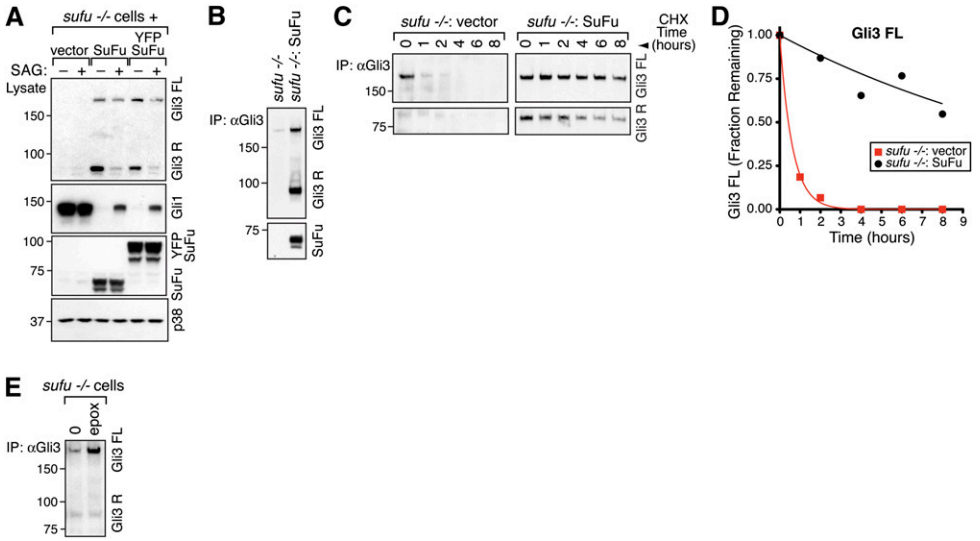

Figure 2. Sufu stabilizes Gli3FL. (*A*) Levels of Gli3FL, Gli3R, Sufu, Gli1 (to assess target gene activation), and p38 (to ensure equal loading) were assayed in *Sufu*$^{-/-}$ cells infected with an empty retrovirus (vector) or with a retrovirus carrying either full-length Sufu or YFP-tagged Sufu. Cells were untreated or treated with SAG (100 nM; 12 h). (*B*) Anti-Gli3 immunoprecipitates from whole-cell lysates of *sufu*$^{-/-}$ cells or *sufu*$^{-/-}$ cells rescued with Sufu re-expression (*sufu*$^{-/-}$:Sufu cells) were tested for the presence of Gli3 and Sufu protein by immunoblotting. (*C*,*D*) Gli3FL and Gli3R half-life in the presence or absence or Sufu was measured by treating *sufu*$^{-/-}$:vector cells and *sufu*$^{-/-}$:Sufu cells with cycloheximide (CHX; 100 μg/mL) for the indicated periods of time and then analyzing Gli3FL and Gli3R levels by immunoprecipitation (IP) from whole-cell lysates. Different exposures were necessary for samples from *sufu*$^{-/-}$:vector and *sufu*$^{-/-}$:Sufu cells to prevent signal saturation; equivalent exposures are shown in Supplemental Figure S2A. The fraction of Gli3FL remaining (cf. $t = 0$) in the two cell types is plotted in *D*. (*E*) Gli3FL protein levels in *sufu*$^{-/-}$ cells increase when the proteasome is inhibited with epoxomycin (10 μM; 6 h).

these results suggest that Sufu controls the rate of Gli3R production and not the rate of its degradation.

Low Gli3R production could simply be due to the low amount of Gli3FL substrate available in the absence of Sufu. To address this issue, we overproduced Myc-tagged Gli3FL (Myc-Gli3FL) protein in *sufu*$^{-/-}$ cells. Increasing the levels of Myc-Gli3FL by overexpression did not lead to efficient production of Gli3R unless Sufu was coexpressed (Fig. 3C). The Gli3FL/Gli3R ratio was significantly lower (Fig. 3D) when Sufu was coexpressed, showing that the increase in Gli3R was not simply a consequence of higher levels of Gli3FL protein.

Since PKA is a major regulator of Gli3R production, we tested potential interactions between Sufu and PKA by treating *sufu*$^{-/-}$ cells with Fsk to hyperactivate PKA. Fsk treatment modestly increased the amounts of endogenous Gli3R produced in the absence of Sufu (Fig. 3E). However, Fsk was very inefficient at inducing the production of Gli3R from endogenous Gli3FL in the absence of Sufu. The levels of Gli3R in Fsk-treated *sufu*$^{-/-}$ cells remained far below those seen in *sufu*$^{-/-}$:Sufu cells (Fig. 3E; Supplemental Fig. S3C). In fact, the small amount of Gli3R induced by Fsk in *sufu*$^{-/-}$ cells was insufficient to extinguish target gene transcription (Fig. 3F; Supplemental Fig. S3C). Thus, Sufu may play an important role in enhancing the ability of PKA to promote the processing of Gli3FL to Gli3R.

How could Sufu have such a dramatic effect on the half-life of Gli3FL but little effect on the half-life of Gli3R? One possibility is that Sufu binds only to the full-length protein but not to the truncated repressor fragment. Previous experiments using overexpressed or purified proteins showed that Sufu binds to both N-terminal and C-terminal regions of Gli3 (Pearse et al. 1999; Dunaeva et al. 2003). We re-examined the association between Gli3 and Sufu, this time testing the interaction between endogenous proteins in extracts made from NIH3T3 cells. Immunoprecipitation of both Gli3FL and Gli3R from these extracts with an anti-Gli3 antibody pulled down Sufu, as predicted if Gli3 and Sufu proteins exist in a complex (Fig. 3G). Since the anti-Gli3 antibody recognizes Gli3FL and Gli3R, we could not determine whether Sufu interacts with one or both Gli3 proteins. However, when Sufu was immunoprecipitated from extracts with anti-Sufu, only Gli3FL coprecipitated with Sufu (Fig. 3G). Gli3R did not coprecipitate with Sufu, even though it was present at much higher levels. To exclude the possibility that our polyclonal anti-Sufu antibody disrupted the Sufu–Gli3R complex, we used an anti-YFP antibody to isolate YFP-Sufu from *sufu*$^{-/-}$ cells rescued with stable expression of YFP-Sufu. Again, Gli3FL but not Gli3R coprecipitated, in concordance with our results using the anti-Sufu antibody (Fig. 3H). Thus, Gli3R and Sufu likely exist in separate complexes in cells.

The simplest model consistent with the above data is that the Gli3FL–Sufu complex is the best substrate for the processing reaction that produces Gli3R. Once Gli3R is generated, it is released from Sufu and presumably enters the nucleus to repress target genes. Cell fractionation experiments described below showed Gli3R to reside mainly in the nucleus (Fig. 5A).

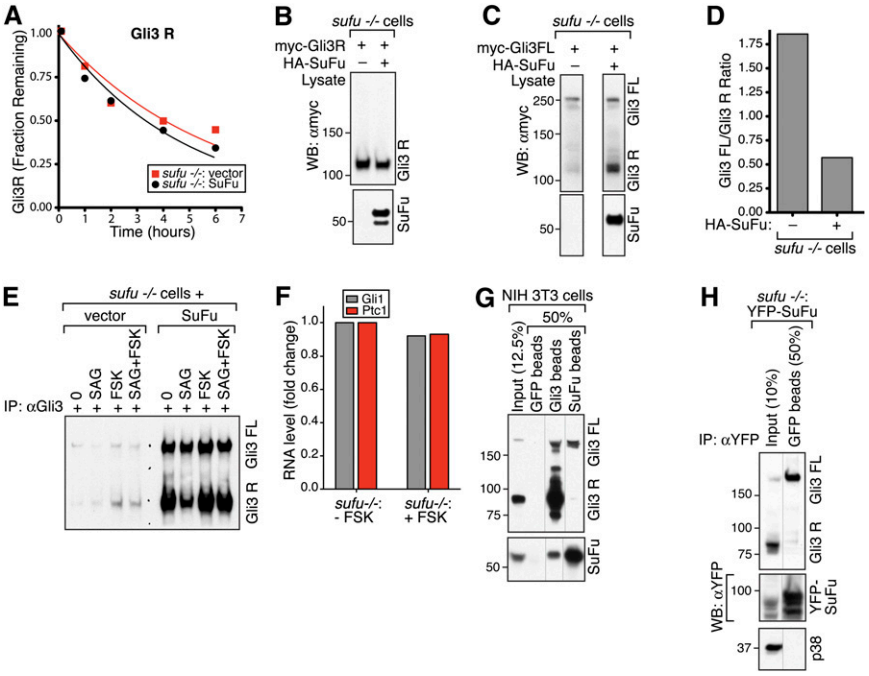

Figure 3. Sufu promotes the synthesis but does not affect the degradation of Gli3R. (*A*) Fraction of Gli3R remaining in either *sufu*$^{-/-}$:vector cells or *sufu*$^{-/-}$:Sufu cells after treatment with cycloheximide (CHX; 100 μg/mL). (*B*,*C*) Analysis of Gli3 and Sufu protein levels in *sufu*$^{-/-}$ cells transiently transfected (72 h) with Myc-Gli3R (*B*) or Myc-Gli3FL (*C*), either alone or in combination with HA-tagged Sufu. (*D*) Gli3FL and Gli3R levels from *C* were quantitated by densitometry and used to calculate the Gli3FL/Gli3R ratio. (*E*) Levels of Gli3FL and Gli3R are much higher in *sufu*$^{-/-}$:Sufu cells compared with *sufu*$^{-/-}$:vector cells under the treatment conditions listed (6 h; SAG, 100 nM; Fsk, 20 μM). Since the signal from *sufu*$^{-/-}$:Sufu samples is saturated, a lower exposure is shown in Supplemental Figure S3C. (*F*) RNA levels of the Hh target genes *Gli1* or *Ptc1* measured by quantitative RT–PCR in *sufu*$^{-/-}$ cells treated with Fsk (20 μM). (*G*,*H*) Lysates from NIH3T3 cells (shown in *G*) were incubated with control beads (anti-GFP), anti-Gli3 beads, or anti-Sufu beads, and the amount of Gli3 and Sufu captured was determined by immunoblotting. (*H*) Only Gli3FL but not Gli3R is coprecipitated with YFP-Sufu from lysates of *sufu*$^{-/-}$:YFP-Sufu cells incubated with anti-YFP beads. In *G* and *H*, all of the lanes are at equivalent exposures from the same immunoblot; light-gray lines separate nonadjacent lanes that have been juxtaposed for clarity.

Hh signaling triggers the dissociation of Gli3FL and Gli2FL from Sufu

The dramatic effect of Sufu on the stability of Gli3FL (Fig. 2) led us to consider the possibility that the decline in Gli3FL stability seen when Hh signaling is activated (Fig. 1) was caused by the release of Gli3FL from Sufu. A recent report stated that there was no decrease in the Sufu–Gli interaction in response to Shh (Chen et al. 2009), but that experiment was done using overproduced quantities of both proteins that could have escaped limiting regulatory mechanisms in the cell.

The interaction between endogenous Gli3 and Sufu was tested by immunoprecipitating Gli3 from extracts made from NIH3T3 cells treated with SAG for increasing amounts of time. As expected, SAG treatment led to a decline in total Gli3FL levels (Fig. 4A). More interestingly, the amount of Sufu that coprecipitated with Gli3FL showed a time-dependent decline after initiation of signaling (Fig. 4A; Supplemental Fig. S4A). The amount of Sufu detected in Gli3 immunoprecipitates could decline simply because the total level of Gli3FL protein is decreasing, not because there is a change in association. This is not the case, for two reasons. First, the Sufu/Gli3FL ratio (Fig. 4B), which is proportional to the amount of Sufu pulled down per unit of Gli3FL, showed a time-dependent decline. Second, the amount of Sufu that coprecipitated with Gli3FL decreased in response to signaling even when Gli3FL degradation was prevented by treatment with the proteasome inhibitor MG132 (Fig. 4A,B).

We also examined if the signal-induced dissociation of Sufu from Gli3FL association also held for Gli2FL, often considered the major transcriptional activator in cells. Since we did not have antibodies to immunoprecipitate Gli2, we instead isolated endogenous Sufu and tested for the amount of coprecipitated Gli2 by immunoblotting. Similar to Gli3, the amount of endogenous Gli2 that precipitated with Sufu showed a time-dependent decline in response to SAG (Fig. 4C,D).

Fsk prevented both the decline in Gli3FL and the decline in Gli3R seen in response to Hh signaling (Fig. 1C). If Sufu association controls both events, an important prediction is that Fsk should block the SAG-induced dissociation of Gli3 and Sufu. Pretreatment of cells with Fsk completely blocked the SAG-induced dissociation of Gli3 and Sufu, as measured by the absolute levels of Sufu coprecipitated with Gli3 and by the Sufu/Gli3 ratio (Fig. 4E,F; Supplemental Fig. S4B).

Hh signaling leads to the phosphorylation and nuclear translocation of Gli3FL

A long-standing question in Hh signaling is how full-length Gli proteins are converted into transcriptional activators. A transcriptional activator must enter the nucleus to stimulate the transcription of target genes. Subcellular fractionation was used to determine the localization of endogenous Gli3 and Sufu in NIH3T3 cells without Hh pathway activation. Gli3FL and Sufu were found predominantly in the cytoplasm, while Gli3R was located in the nucleus (Fig. 5A). The presence of Sufu in the same compartment as Gli3FL but in a different compartment than Gli3R is in agreement with our observation that Sufu associates with Gli3FL but not Gli3R (Fig. 3G). It is also consistent with

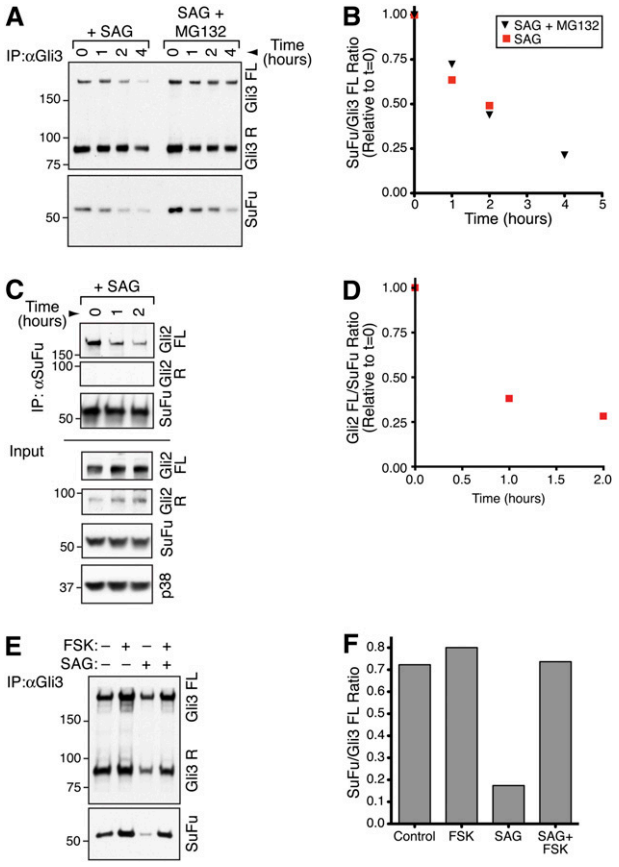

Figure 4. Hh signaling promotes the dissociation of Sufu from Gli3FL and Gli2FL. (*A*) A time-dependent decrease in the amount of Sufu that coprecipitates with Gli3 from lysates of NIH3T3 cells treated with SAG alone (100 nM) or SAG + MG132 (25 μM). MG132 was added 30 min before SAG. (*B*) A time-dependent decrease in the amount of Sufu pulled down per unit of Gli3FL, estimated using the ratio of the Sufu signal to the Gli3FL signal from *A*. (*C*,*D*) A time-dependent decrease in the amount of Gli2FL that coprecipitates with anti-Sufu beads from lysates of NIH3T3 cells treated with SAG (100 nM) for the indicated periods of time. (*E*,*F*) Fsk (20 μM) prevents the SAG-induced dissociation (100 nM; 6 h) of Sufu from Gli3, assayed by determining the amount of Sufu that coprecipitated with anti-Gli3 beads from NIH3T3 lysates (shown in *E*). (*F*) The ratio of the Sufu signal to the Gli3FL signal from *E* was plotted.

a previous report that Gli3FL and Sufu are both localized in primary cilia, but Gli3R is found only in the nucleus (Haycraft et al. 2005).

In response to Smo activation by SAG, Gli3FL shifted from the cytoplasm to the nucleus, assessed by either absolute levels of Gli3FL in the nucleus (Fig. 5B) or the calculated fraction of total Gli3FL in the nucleus (Fig. 5C). Gli2FL also moved from the cytoplasm to the nucleus in response to SAG (Supplemental Fig. S5A), although total Gli2 levels remained stable after signal activation (Supplemental Fig. S5C). In contrast, Sufu, Gli3R, and the standing pool of Gli1 did not show any change in subcellular localization in response to SAG (Fig. 5B; Supplemental Fig. S5A). The rise in nuclear Gli3FL was caused by increased nuclear import rather than decreased nuclear export because Leptinomycin B, an inhibitor of nuclear export, did not enhance Gli3FL accumulation in the nucleus (Supplemental Fig. S5B).

The activation of Hh signaling led to both the nuclear translocation and destabilization of Gli3FL. These changes in the biochemical properties of Gli3FL may reflect its conversion into a transcriptional activator (Gli3A), since the activation of transcription factors is often coupled to their degradation (Collins and Tansey 2006). To determine whether the signal-induced nuclear translocation of Gli3FL is coupled to its degradation, cells were treated with SAG and the proteasome inhibitor MG132. MG132 stabilized Gli3FL in the nucleus, but had little effect on Gli3FL in the cytoplasm (Fig. 5B,C). This suggested that Gli3FL is degraded in the nucleus, after Hh signaling drives its movement from the cytoplasm. To directly follow the dynamics and dissect the temporal order of Gli3FL nuclear translocation and degradation, levels of Gli3FL in the nucleus and cytoplasm were assessed at various times after SAG addition (Fig. 5D,E). The rapid decline in cytoplasmic Gli3FL was accompanied by a concomitant increase in nuclear Gli3FL, showing that the initial event was translocation from the cytoplasm to the nucleus. This was followed by the degradation of the nuclear pool of Gli3FL. Notably, nuclear translocation of Gli3FL (<30 min) occurs before target gene transcripts can be detected (>2 h) (Fig. 1B).

The above studies support the view that the activator form of Gli3 is a labile species localized in the nucleus. This instability may be the reason that it has been difficult to detect endogenous Gli3 (and Ci155) in the nucleus after activating the pathway, especially when looking at late time points after signal initiation. In searching for a biochemical mark that might distinguish Gli3A from Gli3FL, we observed that Gli3FL extracted from the nucleus after treatment with SAG consistently migrated more slowly on SDS-PAGE gels compared with either cytoplasmic Gli3FL or nuclear Gli3FL extracted in the absence of SAG (Fig. 5B,F). The gel migration difference suggested that nuclear Gli3FL was phosphorylated selectively in a signal-regulated manner.

The phosphorylation of Gli3FL induced by Smo activation was unexpected because previous work had suggested that GliFL (and Ci155) proteins are dephosphorylated in response to signaling (Chen et al. 1999). Since we observed the opposite, Gli3FL was analyzed carefully using two different techniques to establish that the gel shift observed in the nuclear fraction was indeed caused by phosphorylation rather than a different post-translational modification. First, we used phosphate affinity SDS-PAGE (Kinoshita et al. 2009), a method in which gels incorporate Mn^{+2}-Phos-tag. This dinuclear metal complex binds selectively to phosphomonoesters, and thus enhances only those gel shifts caused by phosphorylation events on proteins. The mobility of Gli3FL extracted from the nuclei of SAG-treated cells was significantly retarded on gels containing Phos-tag when compared with identical gels lacking Phos-tag (Fig. 5G). The mobility of nuclear Gli3FL from SAG-treated cells was much slower than the mobility of cytoplasmic Gli3FL or the mobility of nuclear

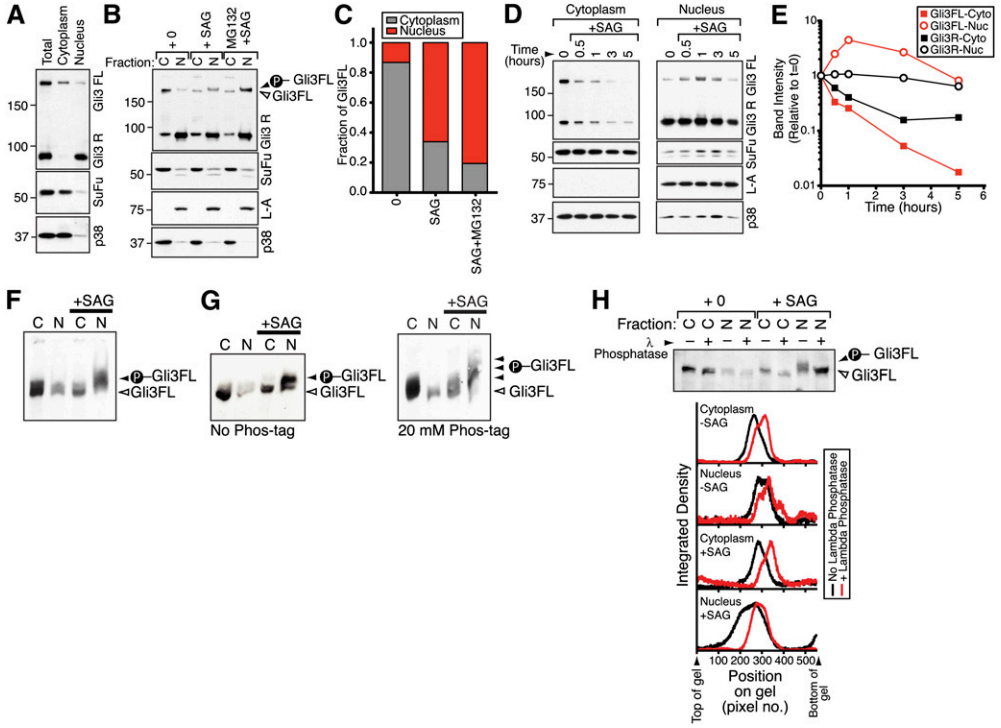

Figure 5. Hh signaling promotes the nuclear translocation, phosphorylation, and degradation of Gli3FL. (*A*) Subcellular fractionation reveals that Gli3FL, Sufu, and p38 are localized predominantly in the cytoplasm (C) while Gli3R is localized in the nucleus (N). Total (T) denotes a whole-cell extract. (*B*) NIH3T3 cells were left untreated, treated with SAG alone (100 nM), or SAG + MG132 (25 μM) for 2 h. Gli3FL, Gli3R, and Sufu protein levels were determined separately in nuclear (N) and cytoplasmic (C) fractions. In this and subsequent experiments, Lamin A (L-A) and p38 serve as control nuclear and cytoplasmic proteins to assess the quality of the fractionation. The fraction of Gli3FL in the cytoplasm or nucleus for each of the conditions shown in *B* is plotted in *C*. (*D*,*E*) Time courses showing changes in Gli3FL and Gli3R levels in the nucleus or the cytoplasm after stimulation with SAG (100 nM). Gli3FL and Gli3R levels from the immunoblot in *D* are plotted in *E*. (*F*) The electrophoretic mobility of Gli3FL present in the nucleus is slower after SAG treatment (100 nM, 2 h) when assessed on a 5% SDS-PAGE gel run for 12 h at 4°C. (*G*) Gels (3.5% acrylamide/0.5% agarose) without (*left*) or with (*right*) Mn^{+2}-Phos-tag acrylamide show that the presence of Phos-tag retards the electrophoretic mobility of Gli3FL. (*H*) The mobility of Gli3FL in the nuclear and cytoplasmic fractions of cells treated with SAG (100 nM; 2 h) or left untreated. Each sample was treated with λ phosphatase (+) or a buffer control (−) to assess for phosphorylation. (*Bottom*) To easily visualize differences in mobility, the signal in each lane was plotted as a function of position.

Gli3FL in the absence of SAG (Fig. 5G), demonstrating that Gli3FL found in the nucleus in response to signaling has a unique pattern of phosphorylation. Second, the reduced mobility of nuclear Gli3FL seen in response to signaling could be reversed by λ phosphatase treatment (Fig. 5H), providing independent evidence for phosphorylation. Plots of Gli3FL mobility (Fig. 5H) suggested that cytoplasmic Gli3FL was also likely phosphorylated; however, the mobility, and hence the phosphorylation pattern, of nuclear Gli3FL was clearly different after SAG addition. In summary, conversion of Gli3 into a transcriptional activator was associated with its nuclear translocation, differential phosphorylation, and destabilization.

PKA is thought to inhibit both mammalian and *Drosophila* Hh signaling primarily by promoting formation of Gli3R (Wang et al. 2000; Smelkinson et al. 2007). However, PKA activation stabilized Gli3FL (Fig. 1C), so we considered the possibility that PKA may also inhibit conversion of Gli3FL into Gli3A. Treatment of cells with Fsk inhibited the SAG-induced nuclear translocation (Figs. 6A; Supplemental Fig. S6A), phosphorylation (Supplemental Fig. S6A), and degradation of Gli3FL (Supplemental Fig. S4B). These results are consistent with the ability of Fsk to prevent the signal-induced dissociation of Sufu from Gli3FL (Fig. 4). To test whether the ability of PKA to inhibit formation of Gli3A influenced target gene transcription, cells were treated simultaneously with Shh and Fsk. Under these conditions, *Gli1* was transcribed in a short pulse, presumably because the rapid activation of *Gli1* transcription by Shh was followed by the slower kinetics of Fsk action (Fig. 6B). This pulse was mirrored by changes in the level of Gli3FL, with unstable Gli3FL associated with high transcription and stable Gli3FL associated with low transcription (Fig. 6B). During this experiment, Fsk inhibited *Gli1* and *Ptc1* transcription without increasing the levels of Gli3R. These experiments confirm that the unstable form of Gli3FL is a transcriptional activator, and that PKA can inhibit target gene induction by preventing the conversion of Gli3FL into Gli3A.

To dissect the relationship between Sufu dissociation, nuclear translocation, phosphorylation, and degradation, we took advantage of the observation that disruption of

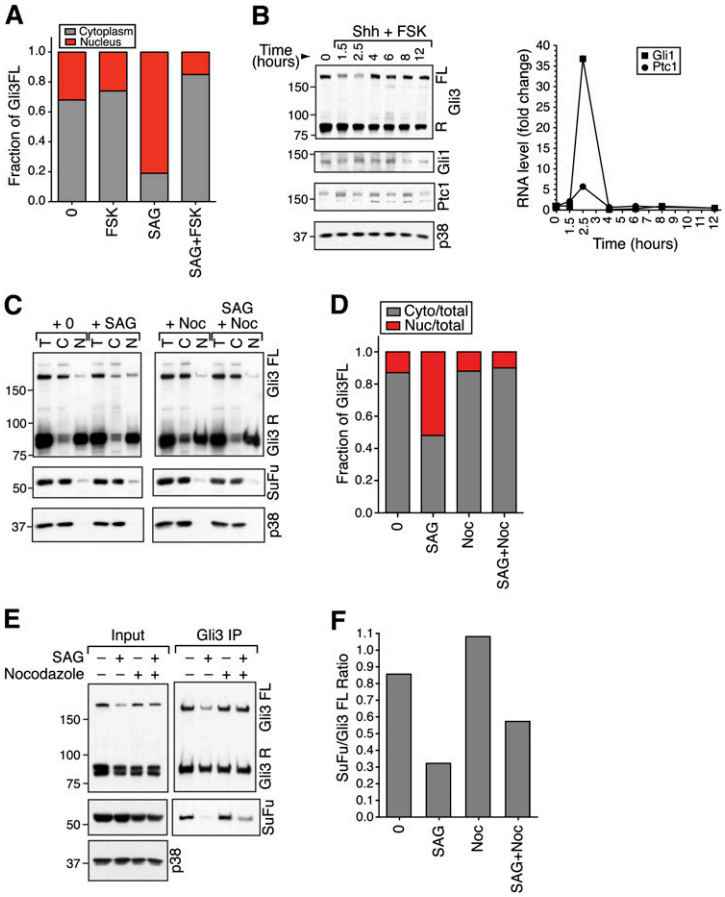

Figure 6. PKA activation blocks the nuclear translocation of Gli3FL. (*A*) Fsk (20 μM) blocks the SAG-induced translocation of Gli3FL from the cytoplasm to the nucleus. The plots are derived from immunoblots shown in Supplemental Figure S6A (*B*) NIH3T3 cells were treated with Fsk (10 μM) + Shh at t = 0, Gli3FL and Gli3R proteins levels were measured by immunoblotting (*left*), and target gene transcription was assessed by *Gli1* and *Ptc1* mRNA levels measured by quantitative RT–PCR (*right*). Nocodazole (15 μM) blocks SAG-induced (100 nM, 3 h) phosphorylation (*C*), nuclear translocation (*C*,*D*), and degradation (*E*) of Gli3FL. However, nocodazole cannot prevent the SAG-triggered dissociation of Sufu from Gli3FL, assayed with an anti-Gli3 IP (*E*, *right* panel) and quantitated as the amount of Sufu pulled down per unit of Gli3FL (*F*).

cytoplasmic microtubules blocks nuclear translocation of Gli2 (and target gene transcription) in response to Hh signaling (Kim et al. 2009). As for Gli2, the SAG-induced nuclear translocation of Gli3FL could be blocked by the microtubule-disrupting agent nocodazole (Fig. 6C,D; Supplemental Fig S6B). While nocodazole treatment also blocked the SAG-induced phosphorylation (Fig. 6C) and destabilization (Fig. 6E) of Gli3FL, it did not prevent the dissocation of Sufu from Gli3FL (Fig. 6E,F). Thus, cytoplasmic microtubules appear to be required at a step after Sufu–Gli3 dissociation, but before the coupled processes of nuclear translocation, phosphorylation, and degradation.

Sufu inhibits conversion of Gli3FL into a transcriptional activator

To show that Sufu works by preventing the nuclear translocation and activation of Gli3FL, we examined the subcellular localization of Gli3FL and Gli3R in *sufu*$^{-/-}$ cells. While *sufu*$^{-/-}$ cells have low total levels of Gli3FL (Fig. 2), a large fraction (>50%) of the Gli3FL is localized in the nucleus, consistent with the model that activated Gli proteins are highly unstable and are located in the nucleus (Fig. 7A,B). Gli3FL in nuclei of *sufu*$^{-/-}$ cells also migrated more slowly on SDS-PAGE gels than the Gli3FL present in the cytoplasm, suggestive of differential phosphorylation (Supplemental Fig. S7A). When Gli3FL degradation was inhibited with MG132 in *sufu*$^{-/-}$ cells, all of the additional Gli3FL accumulated in the nucleus (Fig. 7A,B). This supports the idea that Gli3A was degraded in the nucleus, either when Sufu protein was missing (Fig. 7A) or when Gli3FL was released from Sufu in response to Hh signaling (Fig. 5). The reintroduction of Sufu into *sufu*$^{-/-}$ cells extinguished target gene transcription and stabilized Gli3FL (Fig. 2A). Importantly, Sufu restoration into *sufu*$^{-/-}$ cells dramatically reduced the fraction of Gli3FL in the nucleus, despite the fact that the total level of Gli3FL was much higher in the presence of Sufu (Fig. 7C,D). Unlike Gli3FL, Gli3R was localized predominantly in the nucleus in the presence or absence of Sufu (Fig. 7C).

In summary, Gli3FL in *sufu*$^{-/-}$ cells has the same biochemical characteristics—nuclear location, instability, and differential phosphorylation—as wild-type fibroblasts treated with SAG, which both activates signaling and triggers the dissociation of Gli3 from Sufu. This finding provides an explanation for how *sufu*$^{-/-}$ cells can attain high target gene transcription despite containing low levels of Gli2 and Gli3 (Chen et al. 2009). Thus, Sufu inhibits Hh signaling in the cytoplasm by preventing conversion of Gli3FL into a transcriptional activator.

Dissociation of the Sufu–Gli3 interaction depends on the ciliary motor Kif3a

Cells and embryos with defective primary cilia are impaired in the production of activator and repressor forms

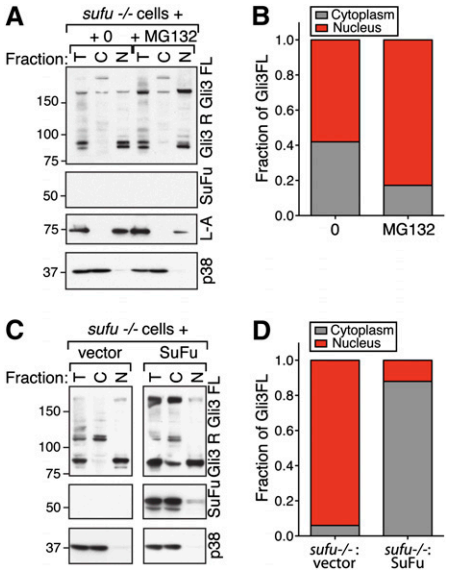

Figure 7. Sufu prevents the nuclear translocation of Gli3FL. Immunoblot (*A*) and graph (*B*) of Gli3FL from the subcellular fractionation of *sufu*$^{-/-}$ cells untreated or treated with MG132 (25 μM; 4 h). (*C*,*D*) Immunoblot (*C*) and graph (*D*) showing levels of total (T), cytoplasmic (C), and nuclear (N) Gli3FL in *sufu*$^{-/-}$: vector cells or *sufu*$^{-/-}$:Sufu cells. While the Gli3FL stabilized by MG132 in *A* was located in the nucleus, the Gli3 stabilized by Sufu readditon is located in the cytoplasm.

of the Gli proteins (Huangfu and Anderson 2006). The requirement for cilia was established by genetic studies in mice, and a large decrease in Gli3R was observed in lysates of embryos with ciliary defects (Huangfu and Anderson 2005; Liu et al. 2005).

Elucidation of the means by which Sufu regulates the formation of Gli3A and Gli3R provided an opportunity to learn which biochemical step is influenced by primary cilia. We used a mouse fibroblast cell line made from embryos lacking the anterograde IFT motor Kif3a (*kif3a*$^{-/-}$ cells), which has been used previously to study the role of primary cilia in Hh and Wnt signaling (Corbit et al. 2008; Chen et al. 2009). *Kif3a*$^{-/-}$ mice have severe defects in primary cilia and have phenotypes consistent with impaired Hh signaling (Huangfu et al. 2003; Huangfu and Anderson 2005; Liu et al. 2005). The steady-state level of Gli3FL was similar in both *kif3a*$^{-/-}$ and *kif3a*$^{+/+}$ cells, but *kif3a*$^{-/-}$ cells had a significantly lower level of Gli3R (Fig. 8A). However, Gli3FL failed to translocate to the nucleus in *kif3a*$^{-/-}$ cells treated with SAG (Fig. 8A,B; Supplemental Fig. S8A). In addition, SAG treatment of *kif3a*$^{-/-}$ cells did not induce the phosphorylation of nuclear Gli3FL typically seen in wild-type cells (Supplemental Fig. S8A). In control *kif3a*$^{+/+}$ cells, SAG-induced nuclear translocation and phosphorylation of Gli3FL was maintained (Figs. 8A; Supplemental Fig. S8A). These data provide direct biochemical evidence that Kif3a is required for the activation of full-length Gli proteins, and support genetic experiments showing that mouse embryos with damaged cilia cannot produce activator forms of the Gli proteins (Huangfu and Anderson 2005; Liu et al. 2005).

We next tested the association between Gli3 and Sufu in both *kif3a*$^{+/+}$ and *kif3a*$^{-/-}$ cells. In the absence of pathway stimulation, the Gli3–Sufu interaction was readily detected in cells from both genotypes (Fig. 8C), and the amount of Sufu precipitated per unit of Gli3FL (the Sufu/Gli3 ratio) derived from Gli3 immunoprecipitates was similar in both cell types (Fig. 8D). This supports the idea, presented in two recent studies, that primary cilia are not required for Sufu to inhibit Gli proteins (Chen et al. 2009; Jia et al. 2009). We next analyzed how the Gli3–Sufu interaction changed after Hh pathway activation. SAG caused the dissociation of Gli3FL from Sufu in *kif3a*$^{+/+}$ cells, but SAG was unable to induce the dissociation of Gli3FL from Sufu in cells lacking *kif3a*$^{-/-}$ (Fig. 8C,D). Thus, the ability of Hh signaling to disrupt the Sufu–Gli3 interaction depends on Kif3a. Indeed, this is likely to be the major function of Kif3a and primary cilia in Hh signaling, because Kif3a is dispensable for target gene transcription in *sufu*$^{-/-}$ cells (Supplemental Fig. S8B; Chen et al. 2009).

Discussion

The main goal of Hh signaling is to alter the transcriptional program of the cell by influencing the balance between the activator and repressor functions of the Gli proteins. The dissociation of Sufu from Gli3 coordinately accomplishes the two main tasks of Hh signaling: inhibition of Gli3R formation, and promotion of Gli3A formation. We present our model for how the Sufu–Gli interaction, likely regulated by biochemical

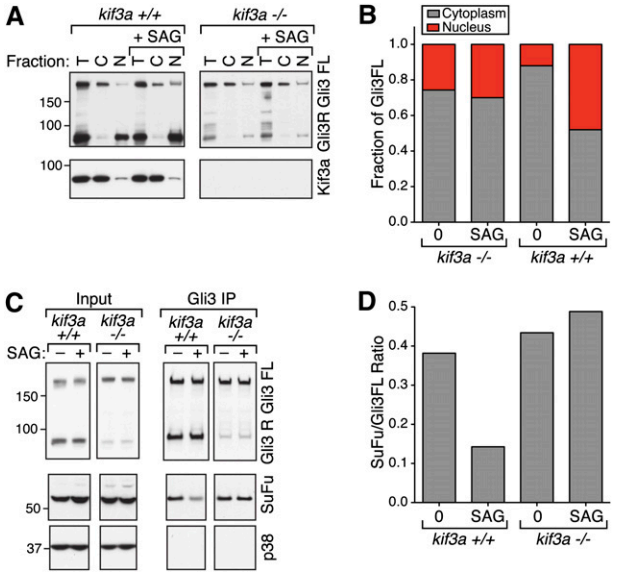

Figure 8. Kif3a is required for Hh-induced dissociation of the Sufu–Gli3FL complex and nuclear translocation of Gli3FL. (*A*,*B*) Subcellular fractions generated from *kif3a*$^{+/+}$ or *kif3a*$^{-/-}$ cells left untreated or treated with SAG (100 nM; 2 h) were assayed for Gli3FL, Gli3R, and Kif3a levels. (*C*,*D*) The amount of Sufu detected in Gli3 immunoprecipitates is unaffected by SAG treatment (100 nM; 2 h) in *kif3a*$^{-/-}$ cells, but drops significantly with SAG treatment in *kif3a*$^{+/+}$ cells, seen both in the immunoblots (*C*) and by changes in the Sufu/Gli3FL ratio (*D*).

events at primary cilia, controls the formation of GliR and GliA.

Gli3R formation

In the absence of Hh signaling, the majority of Gli3FL is processed into Gli3R (Fig. 9A). In mammals, the efficient production of Gli3R depends on the association between Sufu and Gli3FL (Fig. 3). While the association of Gli3FL with Sufu appears to be independent of primary cilia, the subsequent processing of Gli3FL into Gli3R depends on intact cilia (Fig. 8; Huangfu and Anderson 2005). Sufu might promote Gli3 processing by recruiting it to primary cilia, although a recent report showed that overproduced Gli3 localized to cilia in *sufu*$^{-/-}$ cells (Chen et al. 2009). Alternatively, the Gli3FL–Sufu complex may be a better substrate than Gli3FL for the biochemical reactions required for processing (Kise et al. 2009).

Once GliR is produced, its activity is independent of both Sufu and the primary cilium. Gli3R and Sufu proteins do not associate with each other in cells, and reside in separate subcellular compartments. The nuclear localization and half-life of Gli3R are unaffected by the loss of Sufu. The mechanism by which processing of Gli3FL into Gli3R leads to its dissociation from Sufu remains unknown, especially because prior work identified a Sufu-binding region in the N terminus of Gli3 (Pearse et al. 1999; Dunaeva et al. 2003); however, our data suggest that endogenous Gli3R no longer has affinity for Sufu.

Activation of Hh signaling leads to a decrease in the levels of Gli3R, but the mechanism by which this occurs has been unclear in mammals. Our results support the model (Fig. 9B) that the dissociation of Sufu from Gli3FL drives the reduction in Gli3R synthesis seen in response to Hh signaling.

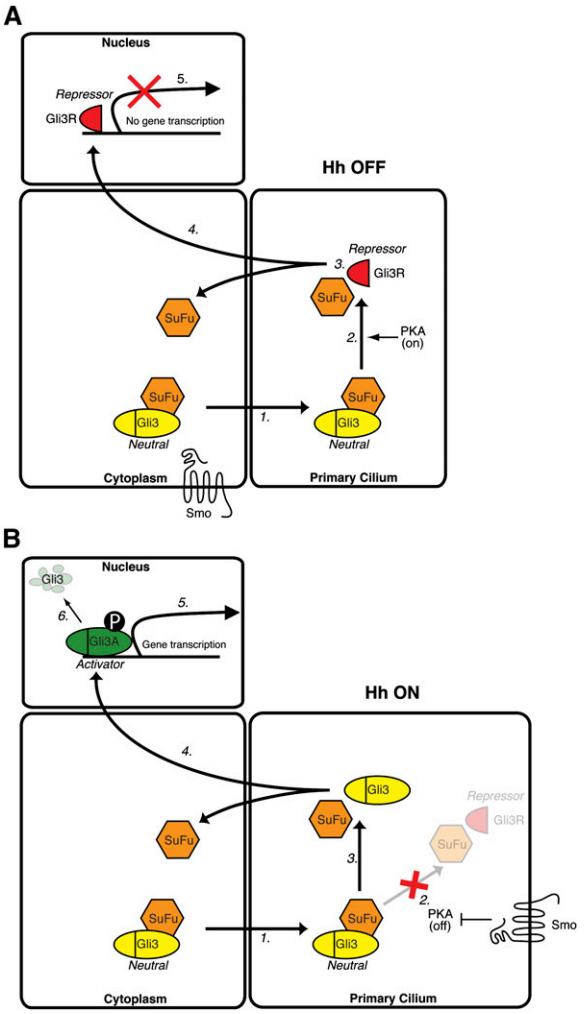

Figure 9. A model for how Sufu association controls the formation of Gli3R and Gli3A. (*A*) Gli3FL is complexed with Sufu in the cytoplasm and is maintained in a neutral state. Without the Hh signal (Hh OFF), the Sufu–Gli3 complex is recruited to cilia (1), leading to the efficient processing of Gli3FL into Gli3R (2). Gli3R formation leads to its dissociation from Sufu (3), allowing Gli3R to translocate into the nucleus (4), and repress Hh target genes (5). (*B*) When Hh signaling is initiated (Hh ON), Sufu dissociates from Gli3FL (3). This has two consequences. First, Gli3R production is halted (2). Second, free Gli3FL translocates to the nucleus (4), where it is phosphorylated, destabilized (6), and converted to a transcriptional activator (5). The level of PKA activity in the cilium may control the relative flux between pathways leading to Gli3R or Gli3A formation.

Gli3A formation

By studying Gli3 in the few hours after SAG treatment, we defined three properties that are associated with an increase in the transcriptional activity of Gli3FL: rapid nuclear translocation, phosphorylation, and destabilization (Fig. 9B). The activity of many transcription factors is often inversely related to their stability, in some cases to limit the duration of transcription, and in other cases because proteolysis is required for efficient transcription (Collins and Tansey 2006). In flies, Hh has been proposed to promote the conversion of Ci155 into a labile transcriptional activator (Ohlmeyer and Kalderon 1998). Thus, the destabilization of Gli3FL in response to signaling might reflect the conversion of Gli3FL to a transient but potent Gli3A. In terms of the mechanism of Gli3 degradation, work in flies and mammals has suggested that Gli3 or Ci155 stability may be regulated by Cul3-based E3 ubiquitin ligases that have a BTB domain-containing substrate recognition module (HIB in flies, SPOP in mammals) (Zhang et al. 2006; Chen et al. 2009).

The phosphorylation of Gli3FL seen after activation of signaling could control degradation, transcriptional activation, or both processes. Differential phosphorylation associated with Gli3A formation is seen only in the nucleus and occurs prior to degradation of Gli3 (Fig. 5D), suggesting that it may be controlled by a nuclear kinase. DYRK1A is a nuclear kinase that has been implicated in the activation of Gli1, but the addition of Harmine, an inhibitor of DYRK1A, had no effect on either nuclear translocation or phosphorylation of Gli3FL (Supplemental Fig. S5B; Mao et al. 2002; Seifert et al. 2008).

Sufu restrains Hh signaling in the cytoplasm

Our study suggests that the main locus for Sufu function in the cell is the cytoplasm, not the nucleus. The majority

of Sufu is present in the cytoplasm, and Sufu does not undergo any change in localization in response to Hh signaling. Experiments in *sufu*$^{-/-}$ cells, along with the observation that the association between Gli3 and Sufu is disrupted by Hh signaling, suggest that the main factor restraining the production of Gli3A is Sufu (Fig. 9B).

The mechanism by which Hh promotes this dissociation of Gli3 from Sufu is a major unresolved question. Some insights into this key step come from the finding that activation of PKA can prevent dissociation of the Gli3FL–Sufu complex, leaving Gli3FL stranded in the cytoplasm and unable to activate target genes. So, a decrease in PKA activity in response to Hh signaling may trigger dissociation of the Sufu–Gli3FL complex. There is some evidence that Smo activation can reduce PKA activity through the inhibitory Gαi class of heterotrimeric G proteins (Riobo et al. 2006; Ogden et al. 2008). The dual involvement of Kif3a and PKA also suggests the interesting hypothesis that Hh signaling regulates Gli3–Sufu association by locally controlling the activity of PKA at the primary cilium (Barzi et al. 2010).

Future prospects

Our study provides a parsimonious model for control of the final, committed step in Hh signal transduction: activation of the Gli family of transcription factors. Unraveling the biochemical details of this activation process is an important goal. In addition, the reactions underlying Gli activation, such as phosphorylation or nuclear translocation, provide novel assays for both basic studies and small molecule and RNAi screens directed against this important pathway.

Materials and methods

Constructs and cell lines

All constructs described in the study were made from mouse genes. NIH3T3 cells were obtained from American Type Culture Collection, *sufu*$^{-/-}$ mouse embryonic fibroblasts (MEFs) were kindly provided by Rune Toftgard (Svard et al. 2006), and *kif3a*$^{+/+}$ and *kif3a*$^{-/-}$ MEFs were kindly provided by Pao-Tien Chuang (Corbit et al. 2008; Wilson et al. 2009). To make *sufu*$^{-/-}$ stable cells with Sufu or YFP-tagged Sufu added back, cDNAs encoding Sufu or Sufu tagged at its N terminus with YFP were cloned into the pRetroX-PTuner retroviral expression vector (Clontech). Retroviral production and infection of *sufu*$^{-/-}$ fibroblasts was performed according to established protocols (Pear et al. 1993). The pRetroX-PTuner vectors include a ligand-responsive destabilization domain; however, this domain could not control Sufu or YFP-Sufu levels, and thus this feature was not used.

Full-length Gli3 (amino acids 1–1583) and Gli3 repressor (amino acids 1–740) were tagged on the N terminus with a 6-myc tag by cloning them into pCS2 + MT, and Sufu was tagged at the N terminus with a 3× HA tag by cloning it into the pCS2 + HA vector.

Cell culture

Cells were grown to confluence in medium (high-glucose DMEM, 0.05 mg/mL penicillin, 0.05 mg/mL streptomycin, 2 mM glutamax, 1 mM sodium pyruvate, 0.1 mM MEM nonessential amino acid supplement) containing 10% FBS (Hyclone, defined grade), and then switched to medium containing 0.5% FBS for 12 h prior to all experiments. Cells were transfected using FugeneHD (Roche) per the manufacturer's instructions.

Small molecules and recombinant proteins

SAG was obtained from Alexis; forskolin was obtained from BIOMOL; puromycin, cycloheximide, and nocodazole were obtained from Sigma; and Leptomycin B was obtained from EMD. The 293 EcR Shh cells (Taipale et al. 2000) were used to produce conditioned media containing processed and lipidated Shh (Supplemental Material). This media was used at a dilution of one to four, with a final FBS concentration of 0.5%.

Antibodies

Anti-Gli1 (mouse monoclonal) was from Cell Signaling Technologies (catalog no. L42B10); anti-Gli2 (goat polyclonal) was from R&D systems (catalog no. AF3635); anti-Gli3 (goat polyclonal) was from R&D systems (catalog no. AF3690); anti-p38, anti-Kif3a, anti-LaminA, and anti-GFP (all rabbit polyclonal) was from Abcam (catalog nos. ab7952, ab11259, ab26300, and ab290); and anti-Myc (9E10, mouse monoclonal) was from Roche. The anti-Sufu polyclonal antibody was produced (Josman Laboratories) in rabbits against full-length mouse Sufu protein and affinity-purified before use. Secondary antibodies conjugated to the horseradish peroxidase enzyme were purchased from Jackson Laboratories. The anti-Ptc1 rabbit polyclonal antibody, produced against a fragment of mouse Ptc1 from amino acids 1169 to 1435, has been described previously (Rohatgi et al. 2007).

Lysate production, immunoprecipitation, and Western blot analysis

For the production of whole-cell lysates, cells were lysed in Buffer A (50 mM Tris at pH 7.4, 300 mM NaCl, 2% NP-40 [v/v], 0.25% Deoxycholate [w/v], 10 mM N-ethyl maleimide, 1 mM DTT, a protease inhibitor cocktail [1× EDTA-free protease inhibitors from Roche]). When cells were treated with MG132 or cycloheximide, these drugs were maintained in the lysis buffers.

For immunoprecipitation, antibodies were coupled covalently to Protein A- or Protein G-coated magnetic beads (Dynal). Anti-Gli3 or anti-Sufu-coupled beads were added to the clarified lysate. After overnight binding at 4°C, the beads were washed with Buffer A and eluted with 2× SDS sample buffer.

Subcellular fractionation

All subcellular fractionation experiments were performed on ice with freshly harvested cells. Cells were washed twice with phosphate-buffered saline (PBS) and twice with 10 mM HEPES (pH 7.4), and then were incubated for 10 min in 10 mM HEPES (pH 7.4). The HEPES buffer was removed and SEAT buffer (10 mM triethanolamine/acetic acid at pH 7.4, 250 mM sucrose, 1× EDTA protease inhibitor cocktail [Roche]) was added. Cells were lysed by 15 passages through a 25-G needle. Nuclei were separated from the post-nuclear supernatant (PNS) by centrifugation at 900*g* for 5 min and then washed once in SEAT buffer. The PNS was also respun at 900*g* for 5 min and then brought to 1× Buffer A, extracted for 1 h, and clarified by centrifugation at 20,000*g* for 1 h. The nuclei were extracted (same conditions as PNS) with 20 mM HEPES (pH 7.9), 1 mM $MgCl_2$, 0.5 M NaCl, 0.2 mM EDTA, 20% glycerol, 1% Triton X-100, 1 mM DTT, benzonase, and a protease inhibitor cocktail. Lysates used for phosphorylation analysis included a phosphatase inhibitor cocktail (1× PhosphoSTOP

[Roche]) except in cases where lysates were treated with λ phosphatase. Extraction volumes for each fraction were equalized before taking samples for gel electrophoresis to ensure that equal amounts of each fraction were loaded on the gel; however, there are always unaccounted losses during fractionation due to the multiple washing and centrifugation steps.

Quantitative real-time PCR

Total cell RNA was isolated using Trizol reagent (Invitrogen) and reverse-transcribed using SuperScript III First Strand Kit (Invitrogen). Real-time PCR (Applied Biosystems 7500) was used to quantify transcript levels. TaqMan gene expression probes (Applied Biosystems) used were Mm00494645_m1 (*gli1*), Mm00970977_m1 (*ptc1*), Mm00492333_m1 (*gli3*), and Mm99999915_g1 (*gapdh* to normalize the samples).

Data analysis

Films were scanned on the Epson Perfection V700 photo scanner into Photoshop at 600 dpi as grayscale TIFF files. Quantitative analysis of band intensities was performed with Total Lab100 (Nonlinear Dynamics), and the data were transferred to GraphPad Prism for normalization, graphing, and curve fitting. All curves shown for the cycloheximide chase experiments represent best-fit single exponential decay curves. To calculate the fraction of Gli3FL in the nucleus or cytoplasm, we calculated the ratios N/N + C and C/N + C, where N is the intensity of the nuclear band and C is the intensity of the cytoplasmic band.

The data presented in the figures are representative of at least three independent experiments, and multiple independent gels are included showing results that support each of the main conclusions in this study. All quantitative comparisons were performed on data obtained within one experiment, because absolute Gli3FL and Gli3R levels were variable from one experiment to another due to differences in cell confluence, cell passage number, and efficiency of immunoblotting. For comparisons, all samples were run on the same SDS-PAGE gel and imaged at identical exposures after immunoblotting.

Phosphorylation analysis

For phosphate affinity electrophoresis, Phos-tag gels containing 3.5% acrylamide (37.5:1 ratio of acrylamide:bis-acrylamide), 0.5% w/v SeaKem Gold agarose (Lonza), 20 μM Phos-tag acrylamide (a kind gift from Nicholas Tilmans and Pehr Harbury), and 40 μM $MnCl_2$ were prepared and run according to a recently published protocol (Kinoshita et al. 2009). For λ phosphatase digestion, cytosolic and nuclear fractions were treated with 1 μL (400 U) of λ protein phosphatase, 1× λ protein phosphatase buffer, and 1 μM $MnCl_2$ for 1 h at room temperature. A 6% (100:1 acrylamide:bis-acrylamide) gel was used for the analysis of λ phosphatase-sensitive gel shifts in Figure 6C.

Acknowledgments

We thank Rune Toftgard for *sufu*$^{-/-}$ cells, Pao-Tien Chuang for *kif3a*$^{-/-}$ and *kif3a*$^{+/+}$ cells, Tyler Hillman and Eunice Lee for advice on Gli3 constructs, Trina Schroer for Kif3a constructs, Maika Deffieu and Suzanne Pfeffer for advice on subcellular fractionation, and Nicholas Tilmans and Pehr Harbury for Phos-tag acrylamide. M.P.S is an Investigator of the Howard Hughes Medical Institute; R.R. is supported by a NCI Pathway to Independence award (K99/ROO CA129174), a V Foundation Scholar award, a SU2C Innovation Award (AACR), and the March of Dimes Basil O'Connor award; and E.W.H is supported by the PanCAN-AACR fellowship, a pilot grant from the Stanford Digestive Disease Center, and the Amgen Hematology-Oncology Fellowship.

References

Aza-Blanc P, Ramirez-Weber FA, Laget MP, Schwartz C, Kornberg TB. 1997. Proteolysis that is inhibited by hedgehog targets Cubitus interruptus protein to the nucleus and converts it to a repressor. *Cell* **89:** 1043–1053.

Barzi M, Berenguer J, Menendez A, Alvarez-Rodriguez R, Pons S. 2010. Sonic-hedgehog-mediated proliferation requires the localization of PKA to the cilium base. *J Cell Sci* **123:** 62–69.

Chen CH, von Kessler DP, Park W, Wang B, Ma Y, Beachy PA. 1999. Nuclear trafficking of Cubitus interruptus in the transcriptional regulation of Hedgehog target gene expression. *Cell* **98:** 305–316.

Chen JK, Taipale J, Young KE, Maiti T, Beachy PA. 2002. Small molecule modulation of Smoothened activity. *Proc Natl Acad Sci* **99:** 14071–14076.

Chen MH, Wilson CW, Li YJ, Law KK, Lu CS, Gacayan R, Zhang X, Hui CC, Chuang PT. 2009. Cilium-independent regulation of Gli protein function by Sufu in Hedgehog signaling is evolutionarily conserved. *Genes & Dev* **23:** 1910–1928.

Cheng SY, Bishop JM. 2002. Suppressor of Fused represses Gli-mediated transcription by recruiting the SAP18–mSin3 corepressor complex. *Proc Natl Acad Sci* **99:** 5442–5447.

Collins GA, Tansey WP. 2006. The proteasome: A utility tool for transcription? *Curr Opin Genet Dev* **16:** 197–202.

Cooper AF, Yu KP, Brueckner M, Brailey LL, Johnson L, McGrath JM, Bale AE. 2005. Cardiac and CNS defects in a mouse with targeted disruption of suppressor of fused. *Development* **132:** 4407–4417.

Corbit KC, Aanstad P, Singla V, Norman AR, Stainier DY, Reiter JF. 2005. Vertebrate Smoothened functions at the primary cilium. *Nature* **437:** 1018–1021.

Corbit KC, Shyer AE, Dowdle WE, Gaulden J, Singla V, Chen MH, Chuang PT, Reiter JF. 2008. Kif3a constrains β-catenin-dependent Wnt signalling through dual ciliary and non-ciliary mechanisms. *Nat Cell Biol* **10:** 70–76.

Ding Q, Fukami S, Meng X, Nishizaki Y, Zhang X, Sasaki H, Dlugosz A, Nakafuku M, Hui C. 1999. Mouse suppressor of fused is a negative regulator of sonic hedgehog signaling and alters the subcellular distribution of Gli1. *Curr Biol* **9:** 1119–1122.

Dunaeva M, Michelson P, Kogerman P, Toftgard R. 2003. Characterization of the physical interaction of Gli proteins with SUFU proteins. *J Biol Chem* **278:** 5116–5122.

Haycraft CJ, Banizs B, Aydin-Son Y, Zhang Q, Michaud EJ, Yoder BK. 2005. Gli2 and Gli3 localize to cilia and require the intraflagellar transport protein polaris for processing and function. *PLoS Genet* **1:** e53. doi: 10.1371/journal.pgen.0010053.

Huangfu D, Anderson KV. 2005. Cilia and Hedgehog responsiveness in the mouse. *Proc Natl Acad Sci* **102:** 11325–11330.

Huangfu D, Anderson KV. 2006. Signaling from Smo to Ci/Gli: Conservation and divergence of Hedgehog pathways from *Drosophila* to vertebrates. *Development* **133:** 3–14.

Huangfu D, Liu A, Rakeman AS, Murcia NS, Niswander L, Anderson KV. 2003. Hedgehog signalling in the mouse requires intraflagellar transport proteins. *Nature* **426:** 83–87.

Jia J, Kolterud A, Zeng H, Hoover A, Teglund S, Toftgard R, Liu A. 2009. Suppressor of Fused inhibits mammalian Hedgehog signaling in the absence of cilia. *Dev Biol* **330:** 452–460.

Kim J, Kato M, Beachy PA. 2009. Gli2 trafficking links Hedgehog-dependent activation of Smoothened in the primary cilium to

transcriptional activation in the nucleus. *Proc Natl Acad Sci* **106:** 12666–21671.
Kinoshita E, Kinoshita-Kikuta E, Koike T. 2009. Separation and detection of large phosphoproteins using Phos-tag SDS-PAGE. *Nat Protoc* **4:** 1513–1521.
Kise Y, Morinaka A, Teglund S, Miki H. 2009. Sufu recruits GSK3β for efficient processing of Gli3. *Biochem Biophys Res Commun* **387:** 569–574.
Liu A, Wang B, Niswander LA. 2005. Mouse intraflagellar transport proteins regulate both the activator and repressor functions of Gli transcription factors. *Development* **132:** 3103–3111.
Lum L, Zhang C, Oh S, Mann RK, von Kessler DP, Taipale J, Weis-Garcia F, Gong R, Wang B, Beachy PA. 2003. Hedgehog signal transduction via Smoothened association with a cytoplasmic complex scaffolded by the atypical kinesin, Costal-2. *Mol Cell* **12:** 1261–1274.
Mao J, Maye P, Kogerman P, Tejedor FJ, Toftgard R, Xie W, Wu G, Wu D. 2002. Regulation of Gli1 transcriptional activity in the nucleus by Dyrk1. *J Biol Chem* **277:** 35156–35161.
Methot N, Basler K. 1999. Hedgehog controls limb development by regulating the activities of distinct transcriptional activator and repressor forms of Cubitus interruptus. *Cell* **96:** 819–831.
Methot N, Basler K. 2000. Suppressor of fused opposes hedgehog signal transduction by impeding nuclear accumulation of the activator form of Cubitus interruptus. *Development* **127:** 4001–4010.
Ogden SK, Fei DL, Schilling NS, Ahmed YF, Hwa J, Robbins DJ. 2008. G protein $G\alpha_i$ functions immediately downstream of Smoothened in Hedgehog signalling. *Nature* **456:** 967–970.
Ohlmeyer JT, Kalderon D. 1998. Hedgehog stimulates maturation of Cubitus interruptus into a labile transcriptional activator. *Nature* **396:** 749–753.
Pastorino L, Ghiorzo P, Nasti S, Battistuzzi L, Cusano R, Marzocchi C, Garre ML, Clementi M, Scarra GB. 2009. Identification of a SUFU germline mutation in a family with Gorlin syndrome. *Am J Med Genet* **149A:** 1539–1543.
Pear WS, Nolan GP, Scott ML, Baltimore D. 1993. Production of high-titer helper-free retroviruses by transient transfection. *Proc Natl Acad Sci* **90:** 8392–8396.
Pearse RV 2nd, Collier LS, Scott MP, Tabin CJ. 1999. Vertebrate homologs of *Drosophila* suppressor of fused interact with the gli family of transcriptional regulators. *Dev Biol* **212:** 323–336.
Preat T. 1992. Characterization of Suppressor of fused, a complete suppressor of the fused segment polarity gene of *Drosophila melanogaster*. *Genetics* **132:** 725–736.
Riobo NA, Saucy B, Dilizio C, Manning DR. 2006. Activation of heterotrimeric G proteins by Smoothened. *Proc Natl Acad Sci* **103:** 12607–12612.
Rohatgi R, Milenkovic L, Scott MP. 2007. Patched1 regulates hedgehog signaling at the primary cilium. *Science* **317:** 372–376.
Seifert A, Allan LA, Clarke PR. 2008. DYRK1A phosphorylates caspase 9 at an inhibitory site and is potently inhibited in human cells by harmine. *FEBS J* **275:** 6268–6280.
Smelkinson MG, Zhou Q, Kalderon D. 2007. Regulation of Ci–SCFSlimb binding, Ci proteolysis, and hedgehog pathway activity by Ci phosphorylation. *Dev Cell* **13:** 481–495.
Stone DM, Murone M, Luoh S, Ye W, Armanini MP, Gurney A, Phillips H, Brush J, Goddard A, de Sauvage FJ, et al. 1999. Characterization of the human suppressor of fused, a negative regulator of the zinc-finger transcription factor Gli. *J Cell Sci* **112:** 4437–4448.
Svard J, Heby-Henricson K, Persson-Lek M, Rozell B, Lauth M, Bergstrom A, Ericson J, Toftgard R, Teglund S. 2006. Genetic elimination of Suppressor of fused reveals an essential repressor function in the mammalian Hedgehog signaling pathway. *Dev Cell* **10:** 187–197.
Taipale J, Chen JK, Cooper MK, Wang B, Mann RK, Milenkovic L, Scott MP, Beachy PA. 2000. Effects of oncogenic mutations in Smoothened and Patched can be reversed by cyclopamine. *Nature* **406:** 1005–1009.
Taylor MD, Liu L, Raffel C, Hui CC, Mainprize TG, Zhang X, Agatep R, Chiappa S, Gao L, Lowrance A, et al. 2002. Mutations in SUFU predispose to medulloblastoma. *Nat Genet* **31:** 306–310.
Tempe D, Casas M, Karaz S, Blanchet-Tournier MF, Concordet JP. 2006. Multisite protein kinase A and glycogen synthase kinase 3β phosphorylation leads to Gli3 ubiquitination by SCFβTrCP. *Mol Cell Biol* **26:** 4316–4326.
Varjosalo M, Taipale J. 2008. Hedgehog: Functions and mechanisms. *Genes & Dev* **22:** 2454–2472.
Wang QT, Holmgren RA. 1999. The subcellular localization and activity of *Drosophila* cubitus interruptus are regulated at multiple levels. *Development* **126:** 5097–5106.
Wang B, Li Y. 2006. Evidence for the direct involvement of βTrCP in Gli3 protein processing. *Proc Natl Acad Sci* **103:** 33–38.
Wang B, Fallon JF, Beachy PA. 2000. Hedgehog-regulated processing of Gli3 produces an anterior/posterior repressor gradient in the developing vertebrate limb. *Cell* **100:** 423–434.
Wilson CW, Nguyen CT, Chen MH, Yang JH, Gacayan R, Huang J, Chen JN, Chuang PT. 2009. Fused has evolved divergent roles in vertebrate Hedgehog signalling and motile ciliogenesis. *Nature* **459:** 98–102.
Zhang W, Zhao Y, Tong C, Wang G, Wang B, Jia J, Jiang J. 2005. Hedgehog-regulated Costal2–kinase complexes control phosphorylation and proteolytic processing of Cubitus interruptus. *Dev Cell* **8:** 267–278.
Zhang Q, Zhang L, Wang B, Ou CY, Chien CT, Jiang J. 2006. A hedgehog-induced BTB protein modulates hedgehog signaling by degrading Ci/Gli transcription factor. *Dev Cell* **10:** 719–729.